Original Article

Institution of MECHANICAL ENGINEERS
Journal of MECHANICAL ENGINEERING SCIENCE

Proc IMechE Part C:
J Mechanical Engineering Science
0(0) 1–12

DOI: 10.1177/0954406214551038
pic.sagepub.com
SAGE

Energy harvesting for powering wireless sensor networks in low-frequency and large-force environments

Xuezheng Jiang[1], Jiong Wang[2], Yancheng Li[3], Jianchun Li[3] and Jin Yao[1]

Abstract

Over the past few decades, wireless sensor networks have been widely used in the field of structure health monitoring of civil, mechanical, and aerospace systems. Currently, most wireless sensor networks are battery powered and it is costly and unsustainable for maintenance because of the requirement for frequent battery replacements. As an attempt to address such issue, this paper theoretically and experimentally studies a compression-based piezoelectric energy harvester, which is suitable for the low-frequency and large-force working environments, such as in civil and transportation infrastructure applications. The proposed energy harvester employs the piezoelectric structure constructed in multilayer stack configuration to convert ambient vibrations into electrical energy. Based on the linear theory of piezoelectricity, the two-degree-of-freedom electromechanical models of the proposed energy harvester were developed to characterize its performance in generating electrical energy under external excitations. Exact closed-form expressions of the electromechanical models have been derived to analyze the maximum harvested power and the optimal resistance. The theoretical analyses were validated through several experiments for a test prototype under harmonic excitations. The test results exhibit very good agreement with the analytical analyses and numerical simulations for a range of resistive loads and input excitation levels.

Keywords

Energy harvesting, low frequency, piezoelectric stack, two-degree-of-freedom electromechanical model

Date received: 28 January 2014; accepted: 19 August 2014

Introduction

Because of the advantages over existing wired technologies, wireless sensor networks have become ubiquitous recently. There is a great interest in leveraging this application in the area of civil and transportation infrastructures by researchers and engineers to collect the real-time data of the infrastructures for the aim of improving the safety and management of the infrastructures. Currently, most wireless electronics are battery powered which is costly for maintenance. The requirement for frequent battery replacements also raises serious reliability and sustainability issues in practice. The battery replacement sometimes can become extremely difficult, particularly in structural health monitoring applications, where hundreds and thousands of sensors are installed during construction stages. For these sensors, if it is not impossible, for the least it is impractical to gain access, remove protection, and replace batteries. Also, the proliferation of wireless sensing devices has stressed even more the need for small power sources as the battery capacity has improved very slowly (by a factor of 2–4 over the last 30 years), while the computational demands for wireless sensors have drastically increased over the same time frame.[1] It is therefore of great necessity to seek alternative power sources for these wireless sensors. In this study, a potential clean and reliable energy source for the wireless sensor networks is developed by scavenging electrical energy from ambient vibrations.

Extracting energy from ambient vibrations is generally known as vibration energy harvesting or vibration energy scavenging. Williams and Yates[2]

[1]School of Manufacturing Science and Engineering, Sichuan University, Chengdu, China
[2]School of Mechanical Engineering, Nanjing University of Science & Technology, Nanjing, China
[3]Centre for Built Infrastructure Research, Faculty of Engineering and Information Technology, University of Technology, Sydney, Australia

Corresponding author:
Xuezheng Jiang, School of Manufacturing Science and Engineering, Sichuan University, No. 24 South Section 1, Yihuan Road, Chengdu 610065, China.
Email: xuezheng.jiang@hotmail.com

have stated that three basic methods, i.e. electromagnetic induction, electrostatic generation, and piezoelectric effect, could be utilized to scavenge electrical energy from ambient vibrations. While each of the aforementioned methods can generate a useful amount of energy, piezoelectric vibration energy harvesters have received more attentions especially in the recent years due to their ability to directly convert applied force into usable electrical charge, as well as its large power density and ease of application.[3–5] Comparing to energy harvesting for large-scale alternative energy generation using wind turbines and solar cells is mature technology, the development of energy harvesting technology by using piezoelectric devices on a scale appropriate for small, low-power, embedded wireless sensing systems is still in its developmental stage, particularly for application of structural health monitoring sensing system.[6] Wischke et al.[7] have investigated the feasibility of harvesting energy from traffic-induced vibrations in railway and road tunnels to power embedded structure health monitoring sensors. They concluded that the traffic-induced vibrations at any location in the road tunnel and at the wall in the railway tunnel are too small for useful vibration harvesting by using the cantilever-based piezoelectric generator. Pasquale et al.[8] proposed a cantilever-based piezoelectric harvester to harvest the vibrations of the railway vehicle's bogie and power a wireless sensor network for the structural monitoring and safety improvement on railway vehicles and have showed good agreement between theoretical analysis and experiment testing. Xie et al.[9] developed a mathematical model to investigate the energy harvesting of a tuned mass damper design made of piezoelectric coupled cantilever attached by a proof mass subjected to vibrations of a high-rise building, and they provided guidance on optimal design of energy harvesting devices made from piezoelectric coupled cantilever structures for the application of high buildings. Of the published results that focus on harvesting energy for the wireless sensor networks in civil and transportation systems, most of them have focused on using the piezoelectric materials constructed in cantilever beam configuration to receive the vibrations and generate electrical energy. The cantilever-based piezoelectric harvester requires working at resonant range to maximum the energy output, which will drop dramatically when the induced frequency is lower than its resonant frequency (normal around 120 Hz).[10] However, the source of vibrations and other dynamic loads in typical civil and transportation infrastructures are usually moving vehicles, walking human, and wind-induced loads and have relatively lower frequency range and cannot meet the requirement of the cantilever-based piezoelectric harvester.[11] Therefore, a medium device is normally needed for the cantilever-based style harvester to match the lower input vibration's frequency with its higher resonant frequency.[12] But the medium device would complicate the whole system and decrease the energy harvesting efficiency.

In this paper, a compression-based piezoelectric harvester was developed in order to scavenge sufficient energy for powering the wireless sensor networks used in the civil and transportation infrastructures. Unlike the cantilever-based harvester, the proposed energy harvester in this paper employs the piezoelectric stack configuration to harvest energy directly from compressive loads, such as vehicular tire forces acting upon pavements. Because the compressive load in civil and transportation systems is usually large enough, the compression-based piezoelectric harvester has the potential ability to harvest sufficient energy for the wireless sensors under the lower frequency condition. The stack configuration is chosen due to its durability for large force excitations and its superior properties on power generation than the single piezoelectric monolithic element.[13] To date, there is limited research reported on the development of stack configuration based piezoelectric harvesters. Keawboonchuay and Engel,[14,15] Platt et al.,[13] and Feenstra et al.[16] have done some feasibility investigations on the piezoelectric harvester in stack configuration, however comprehensive research on the piezoelectric harvester construction in multilayer stack configuration is still limited. Moreover, a piezoelectric harvester system contains two fundamental elements: the mechanical part that generates electrical energy and an electrical circuit that converts and rectifies the generated energy in a form of an alternating voltage into a constant voltage. The efficiency of the energy harvester design depends not only on the piezoelectric harvester itself but also on its integration with the electrical circuit. Therefore, an electromechanical model which considers both the mechanical and electrical aspects of the proposed harvester is of great importance to optimize the design as well as for understanding the behavior of the piezoelectric harvester.

This paper is organized as follows. "Structure design" section briefly introduces the structure of the proposed harvester. "Electromechanical models" section provides the theoretical analysis on the output voltage and power properties of the piezoelectric stack, and develops two two-degree-of-freedom (2DOF) electromechanical models (without and with rectifier circuit) of the proposed piezoelectric energy harvester. Then, lab-scale tests are conducted to experimentally evaluate the theoretical analysis and investigate the energy harvesting capability of the proposed compression-based piezoelectric energy harvester in "Experimental testing." Finally, conclusions from this study are drawn in the final section.

Structure design

The piezoelectric energy harvester proposed in this paper is a compression-based harvesting system,

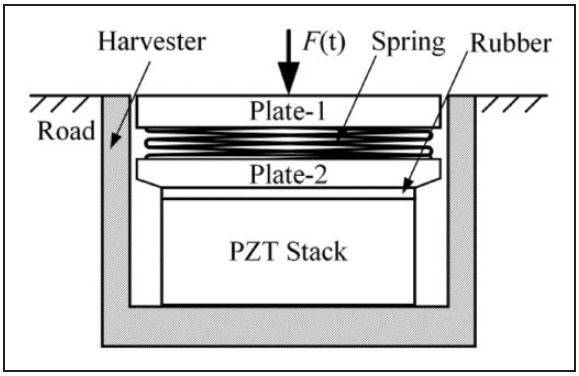

Figure 1. Schematic of the proposed energy harvester.

which employs piezoelectric multilayer stacks to harvest large compressive loads that exist in the field of civil and transportation infrastructure systems application. Figure 1 schematically depicts an example of implementing the proposed harvester for harvesting electrical energy on the road. As shown in Figure 1, the energy harvester is embedded on the surface of the road and will generate electrical energy when a car or a truck passes over. The exciting force, $F(t)$, is the tire force caused by the passing car on the road.

As shown in Figure 1, the proposed energy harvester is a box shaped and chiefly comprised of plate 1, spring, plate 2, hard rubber layer, and a piezoelectric stack. Piezoelectric material is a fragile material and could be broken under large impact forces, such as the impact tire force caused by the passing vehicle. Therefore, it needs to set a medium to endure the large impact force directly and transfer it into endurable time varying force. In this proposed structure, a spring, as shown in Figure 1, is chosen to transfer the large impact tire force into endurable time varying force. Because the spring is in circular structure, two rigid metal plates, i.e. plate 1 and plate 2, were used to endure the tire force directly and make the exciting force exert evenly on the piezoelectric stack, respectively. In addition, there is a hard rubber in this proposed harvester to protect the piezoelectric stack from being damaged. Figure 2 shows the side cross-sectional view of the piezoelectric stack, which is made up of several very thin piezoelectric wafers and electrode elements. In practice, the piezoelectric wafers are polarized along this thickness direction, and all are assembled mechanically in series with alternative polarization direction but connected electrically in parallel to make the stack structure.

When cars pass over, the pressure and vibration caused by the moving vehicle creates time varying forces on the piezoelectric stack, which will generate electrical energy. Electrical energy harvested by the proposed compression-based piezoelectric harvester is proportional to the force applied on the piezoelectric stack, which is determined by the product of the spring's stiffness and compression. Actually, when the structure is determined, the compression of the spring is normally fixed. Therefore, under the maximum

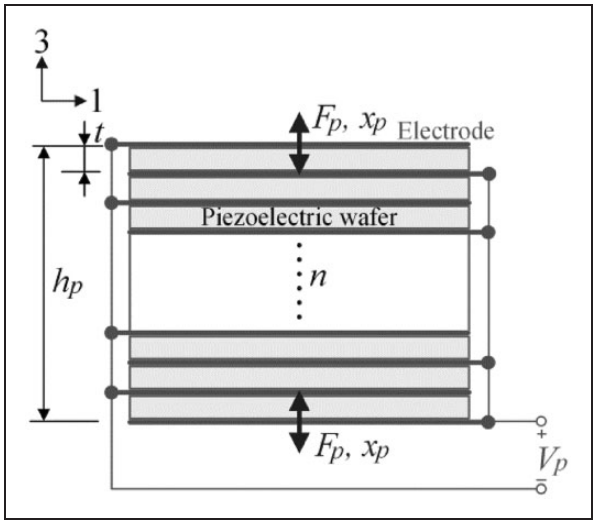

Figure 2. Schematic of the piezoelectric stack.

endurable stress of the piezoelectric material, a spring with large stiffness is normally chosen in order to maximize the force applied on the piezoelectric stack and improve the energy harvesting ability of the proposed piezoelectric harvester. In addition, it needs to be noted that there is a precompression force applied between the piezoelectric stack and plate 1, therefore electricity will still be generated during the rebounding of the compression.

Electromechanical models

Electrical characteristics of the piezoelectric wafer-stack

The proposed harvester employs the piezoelectric stack to scavenge energy from compressive loads. Therefore, for evaluating the energy harvesting capability of the harvester, it is necessary to investigate the electrical characteristics and energy harvesting properties of the piezoelectric stack under external excitation. According to the Institute of Electrical and Electronics Engineers Standard on Piezoelectricity[17,18] under the external force, given by the strain S, stress T, electric field E, and electric displacement D, the constitutive relations of the piezoelectric wafer-stack shown in Figure 1 are typically defined by

$$\begin{bmatrix} T_3 \\ D_3 \end{bmatrix} = \begin{bmatrix} c_3^{\mathrm{E}} & -e_{33} \\ e_{33} & \varepsilon_{33}^{\mathrm{S}} \end{bmatrix} \begin{bmatrix} S_3 \\ E_3 \end{bmatrix} \tag{1}$$

where e_{33} is the piezoelectric coefficient, $c_3{}^{\mathrm{E}}$ is the elastic stiffness constant under a constant electric field, and $\varepsilon_{33}{}^{\mathrm{S}}$ is the dielectric constant under constant strain.

For the piezoelectric stack shown in Figure 2, the parameters in equation (1) can be calculated as

$$S_3 = x_p/h_p,\ E_3 = V_p/t,\ T_3 = F_p/A,\ D_3 = Q/nA \tag{2}$$

where h_p is the height of the stack, A is the cross-section area of the stack, t is the thickness of a single piezoelectric wafer, F_p is the force applied on the stack, x_p is the deformation of the stack under the exciting force, Q is the electric charge generated by the stack, V_p is the output voltage of the stack, and n is the number of piezoelectric wafers used to produce the stack.

In order to simplify the analysis, let the height of the stack be equal to the entire thickness of all the piezoelectric wafers (i.e. $h_p = nt$). Then, substitution of equation (2) into equation (1) yields the constitutive equations of the piezoelectric stack as

$$\begin{bmatrix} F_p \\ Q \end{bmatrix} = \begin{bmatrix} k_p & -N \\ N & C_P \end{bmatrix} \begin{bmatrix} x_p \\ V_p \end{bmatrix} \tag{3}$$

In equation (3), k_p is the elastic coefficient of the stack ($k_p = c_3^{\mathrm{E}} A/h_p$), C_p represents the equivalent capacitance of the stack ($C_p = n\varepsilon_{33}^{\mathrm{S}} A/t$), and N is defined as the electromechanical conversion coefficient of the stack ($N = e_{33} A/t$). The electromechanical conversion coefficient N represents the force–voltage and charge–deformation transferring relation of the stack. From equation (3), a backward force due to piezoelectricity, which actually converts mechanical energy into electrical energy, can be written as

$$F_e = NV_p \tag{4}$$

Equation (4) gives an explicit relationship of external force and output voltage, which will be used to build the electromechanical models of the piezoelectric wafer-stack harvester.

2DOF electromechanical model without a rectifier circuit

In this condition, the electric energy generated by the harvester applies directly on an external resistive load. Considering the mechanical and electrical characteristics of the piezoelectric stack under the external force, the electromechanical model without a rectified circuit of the proposed harvester is illustrated in Figure 3. As shown in Figure 3, F_e is used to link the mechanical parts and electrical parts of the model and convert mechanical energy into electrical energy. The governing equations of the model can be written as

$$\begin{cases} m_r\ddot{y} + c_r\dot{y} + k_r y = F(t) - m_r\ddot{x}_p \\ m_p\ddot{x}_p + c_h\dot{x}_p + k_h x_p + k_p x_p + F_e = F(t) - m_r\ddot{x}_p - m_r\ddot{y} \\ -N\dot{x}_p + C_p\dot{V}_p + \dfrac{V_p}{R} = 0 \end{cases} \tag{5}$$

where y is defined as $y = x_r - x_p$; x_r and x_p are the strain of the rubber and stack under the external force, respectively; m_r, c_r, and k_r are the mass, damping, and elastic coefficient of the rubber, respectively; m_p and k_p are the mass and elastic coefficients of the stack, respectively; c_h and k_h are the mechanical damping and elastic coefficients of the harvester, respectively; I is the current output of the harvester; C_p is the clamped capacitance of the stack; R_p is the piezoelectric leakage resistance and used to represent the electric loss property of the stack; R_l is the external resistive load; and R is the equivalent resistance of two parallel resistances R_p and R_l. In general, R_p is much higher than the load resistance, so that $R \approx R_l$.

Transforming equation (5) into the frequency domain and dividing the first equation by m_r, the second equation by m_p, and the third equation by C_p we obtain

$$\begin{cases} (-\omega^2 + 2\zeta_1\omega_1\omega j + \omega_1^2)Y(\omega) - \omega^2 X_p(\omega) = \dfrac{F(\omega)}{m_r} \\ \left[-(1+\mu)\omega^2 + 2\zeta_2\omega_2\omega j + \omega_2^2\right]X_p(\omega) - \mu\omega^2 Y(\omega) \\ \quad + \dfrac{NV_p(\omega)}{m_p} = \dfrac{F(\omega)}{m_p} \\ -\dfrac{\omega N j X_p(\omega)}{C_p} + (\omega j + \dfrac{1}{RC_p})V_p(\omega) = 0 \end{cases} \tag{6}$$

Here ω is the angular frequency of the vibration and $Y_p(\omega)$, $X_p(\omega)$, $V_p(\omega)$, and $F(\omega)$ are the frequency counterparts of y, x_p, V_p, and $F(t)$. Other parameters, i.e. ω_1, ω_2, ζ_1, ζ_2, μ are defined as

$$\begin{aligned} &\omega_1 = \sqrt{\frac{k_r}{m_r}}, \quad \omega_2 = \sqrt{\frac{k_a}{m_p}}, \quad \zeta_1 = \frac{c_r}{2\sqrt{m_r k_r}}, \\ &\zeta_2 \quad = \frac{c_h}{2\sqrt{m_p k_a}}, \quad \mu = \frac{m_r}{m_p}, \quad k_a = k_p + k_h \end{aligned} \tag{7}$$

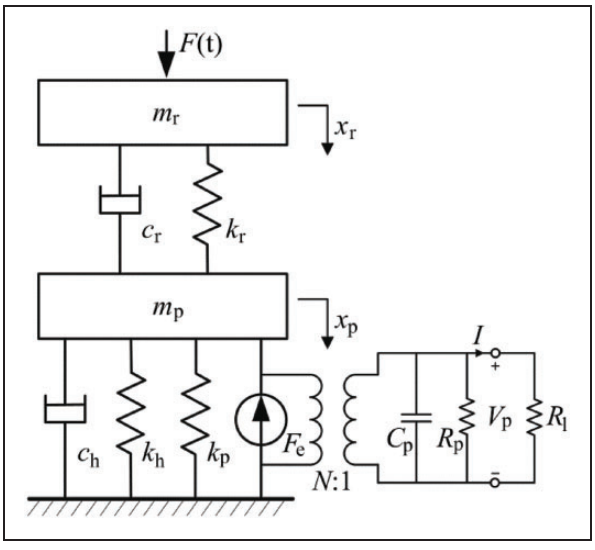

Figure 3. 2DOF electromechanical model without a rectifier circuit.

Solving equation (6) we obtain

$$X_p(\omega)=\frac{\frac{(\alpha^2+2\zeta_1\psi\alpha j)F(\omega)}{k_a(\alpha^2-\psi^2+2\zeta_1\psi\alpha j)}}{1-(1+\mu)\psi^2+2\zeta_2\psi j-\frac{\mu\psi^4}{\alpha^2-\psi^2+2\zeta_1\psi\alpha j}+\frac{\beta\psi k_e^2 j}{1+\beta\psi j}} \tag{8}$$

$$V_p(\omega)=\frac{\frac{(\alpha^2+2\zeta_1\psi\alpha j)F(\omega)}{N(\alpha^2-\psi^2+2\zeta_1\psi\alpha j)}}{\left[1-(1+\mu)\psi^2+2\zeta_2\psi j-\frac{\mu\psi^4}{\alpha^2-\psi^2+2\zeta_1\psi\alpha j}\right]\frac{1+\beta\psi j}{\beta\psi k_e^2 j}+1} \tag{9}$$

where α and ψ are the normalized frequencies, β is the normalized electrical resistance, and k_e is the alternative electromechanical coupling coefficient. Those dimensionless parameters can be calculated as

$$\alpha=\frac{\omega_1}{\omega_2},\quad \psi=\frac{\omega}{\omega_2},\quad \beta=\omega_2 RC_p,\quad k_e^2=\frac{N^2}{C_p k_a} \tag{10}$$

Based on equation (9), the voltage generated by the harvester can be rewritten as

$$V_p(\omega)=\frac{F(\omega)k_e^2\beta\psi\alpha}{N(A_3^2+A_4^2)}\times[(A_3\alpha+2A_4\zeta_1\psi)+(2A_3\zeta_1\psi-A_4\alpha)j] \tag{11}$$

where parameters A3 and A4 can be calculated as

$$\begin{cases} A_3=A_1\beta\psi+(\alpha^2-\psi^2)\beta k_e^2\psi+A_2 \\ A_4=A_2\beta\psi+2\zeta_1\alpha\beta k_e^2\psi^2-A_1 \end{cases} \tag{12}$$

In equation (12), parameters A1 and A2 are defined as

$$\begin{cases} A_1=\alpha^2-\psi^2-(1+\mu)\alpha^2\psi^2+\psi^4-4\zeta_1\zeta_2\psi^2\alpha \\ A_2=2\psi[\alpha(1-\psi^2-\mu\psi^2)\zeta_1+(\alpha^2-\psi^2)\zeta_2] \end{cases} \tag{13}$$

Therefore, based on equation (11), the electrical power generated by the harvester can be calculated as

$$P_1=\frac{V_p\cdot V_p^*}{2R}=\frac{F(\omega)^2k_e^4\beta^2\psi^2\alpha^2[(A_3\alpha+2A_4\zeta_1\psi)^2+(2A_3\zeta_1\psi-A_4\alpha)^2]}{2N^2(A_3^2+A_4^2)^2R} \tag{14}$$

From equation (14), it can be concluded that the electrical power, generated by the presented harvester, depends on the exciting force (frequency ψ and amplitude $F(\omega)$), the mechanical coefficients of the system (such as the natural frequency ω_1 and ω_2, the mechanical damping factor ζ_1 and ζ_2, and the stiffness of the harvester k_a), and the electrical properties of the harvesting system (such as the normalized electrical load β and the overall electromechanical coupling coefficient of the harvester k_e). Also, the value of parameters A_3, A_4, and β is all dependent on the resistive load R, therefore the value of the resistive load has a great impact on the electrical power output of the harvester. It is of great need to find out the optimal external resistive load, on which the power generated by the harvester reaches its maximum value.

Based on equation (14), the optimal resistive load and the maximum electrical power generated by the harvester can be calculated as

$$R_{opt1}=\frac{A}{(A+\alpha^2k_e^2-\psi^2k_e^2)C_p\omega}\quad\text{and}\quad P_{\max 1}=\frac{F(\omega)^2\alpha^4k_e^4C_p\omega}{4N^2A(A+\alpha^2k_e^2-\psi^2k_e^2)} \tag{15}$$

where $A=\alpha^2-\psi^2-(1+\mu)\alpha^2\psi^2+\psi^4$.

Normally, the nature frequency of the piezoelectric wafer-stack is very high (equals to 1.78e4 Hz in this design). Therefore, based on equation (10), it is reasonable to assume that the normalized frequency ψ can be set to zero under low input frequency conditions (lower than 10 Hz). Under this assumption, the optimal resistive load and the maximum generated power can be rewritten as

$$R_{opt1}=\frac{1}{(1+k_e^2)C_p\omega}\quad\text{and}\quad P_{\max 1}=\frac{F(\omega)^2k_e^4C_p\omega}{4N^2(1+k_e^2)}=\frac{F(\omega)^2k_e^2\omega}{4k_a(1+k_e^2)} \tag{16}$$

Equation (16) indicates that the maximum electrical power generated by the proposed piezoelectric harvester is proportional to the frequency of ambient vibration and proportional to the square of the amplitude of ambient vibration. It can also be found that the generated electrical power increases with the electromechanical coupling coefficient k_e. Equation (10) shows that the value of k_e is determined by the mechanical framework of the harvester and the properties of the selected piezoelectric materials. Therefore, careful selection of the piezoelectric material and optimal design of the mechanical structure are very important to obtain higher electromechanical coupling coefficient k_e resulting in optimal scavenging electrical energy under ambient vibration.

Meanwhile, equation (16) shows that the optimal external resistive load for the maximum electrical power generation is not a constant value and changes with the parameters of the harvester, the properties of the piezoelectric material, and the input frequency. The value of the optimal resistive load is inversely

proportional to the input frequency and the capacitance of the piezoelectric material. For a weak electromechanical coupling coefficient k_e, the optimal resistance can be simplified as $1/C_p\omega$.

2DOF electromechanical model with a rectifier circuit

The electrical power generated by the piezoelectric harvester under ambient vibration is normally alternative electricity whose voltage changes with the force excitation caused by the vibrations. In practice, it may be required to convert the alternating voltage output into a constant voltage in order to be used by common low-power electronics. Therefore, rectifier circuit is proposed to convert the generated AC electricity into DC electricity. To analyze the electrical characteristics of the proposed piezoelectric harvester with a rectifier circuit, an electromechanical model with a rectified circuit of the proposed piezoelectric harvester is developed and illustrated in Figure 4. As shown in Figure 4, there is an AC-to-DC rectifier between the harvester and the external resistive load R_l. A filtering capacitance C_r is used to smooth the output DC voltage of the AC-to-DC rectifier. The rectifier bridge is assumed to be ideal in this paper.

Same as equation (5), the governing equations of the model with a rectifier circuit can be presented as

$$\begin{cases} m_r\ddot{y}+c_r\dot{y}+k_r y=F(t)-m_r\ddot{x}_p \\ m_p\ddot{x}_p+c_h\dot{x}_p+k_h x_p+k_p x_p+F_e=F(t)-m_r\ddot{x}_p-m_r\ddot{y} \\ \qquad -N\dot{x}_p+C_p\dot{V}_P+I=0 \end{cases} \tag{17}$$

With regard to the DC output voltage on R_l, if the time constant R_lC_r is much larger compared to the vibration period, the voltage V_r can be considered as a constant. As shown in Figure 4, when $|V_p|$ is lower than V_r, the rectifier is an open circuit, and I and Q are null at this condition. However, when the $|V_p|$ reaches V_r, the rectifier starts to work and the $|V_p|$ is kept equal to the rectified voltage V_r. Finally, the conduction in the rectifier diodes is blocked again when the absolute value of the harvester output voltage $|V_p|$ starts decreasing. Upon the above analysis, the current flowing into the rectified circuit can be calculated as

$$I=\begin{cases} C_r\dot{V}_r+V_r/R_l & \text{if } V_p=V_r \\ -C_r\dot{V}_r-V_r/R_l & \text{if } V_p=-V_r \\ 0 & \text{if } |V_p|<V \end{cases} \tag{18}$$

From equations (17) and (18), it can be found that the voltage output V_p of the harvester with a rectifier circuit varies proportionally with respect to the piezoelectric wafer-stack strain x_p if the rectifier bridge is blocked and the outgoing current is zero. Defining $T=2\pi/\omega$ as the period of the vibration, and t_1 and t_2 as two time instants (t_2–$t_1=T/2$), thus the strain x_p goes from the minimum $-x_{pm}$ to the maximum x_{pm} (x_{pm} is the constant magnitude of the strain). Assume that $\dot{V}_p\geqslant 0$ during the time period from t_1 to t_2, therefore, the integration of the third part of equation (17) from time t_1 to t_2 is

$$-2Nx_{pm}+2C_pV_r+\frac{T}{2}\frac{V}{R_l}=0 \tag{19}$$

Based on equation (19), the rectified voltage V_r can be expressed as a function of the strain amplitude x_{pm}

$$V_r=\frac{2\omega NR_l}{2\omega C_pR_l+\pi}x_{pm} \tag{20}$$

Assume that the external force excitation is independent of the piezoelectric harvester, from equation (8), the strain of the wafer-stack under the external force can be rewritten as

$$X_p(\omega)=\frac{F(\omega)\alpha}{k_a(A_3^2+A_4^2)}(A_5+A_6\,j) \tag{21}$$

where the parameters A_5 and A_6 can be obtained by

$$\begin{cases} A_5=\psi\beta(A_3\alpha+2A_4\zeta_1\psi)+2A_3\zeta_1\psi-A_4\alpha \\ A_6=\psi\beta(2A_3\zeta_1\psi-A_4\alpha)-2A_4\zeta_1\psi-A_3\alpha \end{cases} \tag{22}$$

Based on equation (21), the strain amplitude x_{pm} can be calculated as

$$x_{pm}=\frac{F_m\alpha}{k_a(A_3^2+A_4^2)}\sqrt{A_5^2+A_6^2} \tag{23}$$

where F_m is the amplitude of the external force.

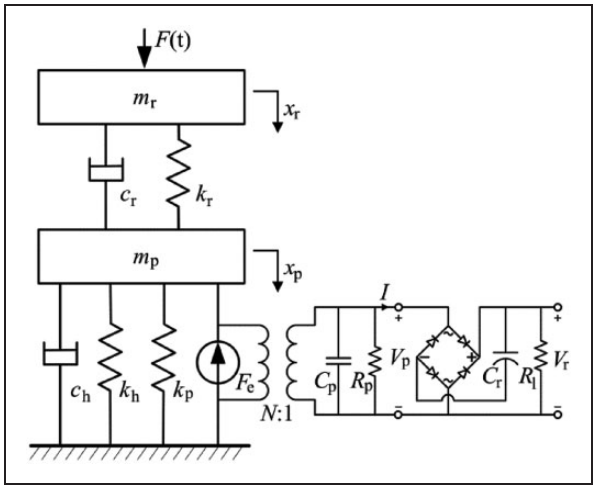

Figure 4. 2DOF electromechanical model with a rectifier circuit.

The rectified voltage under the external resistive load can be rewritten as

$$V_r = \frac{2\omega N R_l}{2\omega C_p R_l + \pi} x_{pm} = \frac{2F_m k_e^2 \beta\psi\alpha\sqrt{A_5^2 + A_6^2}}{N(A_3^2 + A_4^2)(2\psi\beta + \pi)} \tag{24}$$

Based on equation (24), the electrical power under the external resistive load can be expressed as

$$P_2 = \frac{V_r^2}{R_l} = \frac{4F_m^2 k_e^4 \beta^2 \psi^2 \alpha^2 (A_5^2 + A_6^2)}{N^2 (A_3^2 + A_4^2)^2 (2\psi\beta + \pi)^2 R_l} \tag{25}$$

In this case, the maximum harvested electrical power of the harvester and the optimal resistance can be expressed as

$$R_{opt2} = \frac{\pi A}{2(A + \alpha^2 k_e^2 - \psi^2 k_e^2) C_p \omega} \text{ and}$$
$$P_{\max 2} = \frac{F_m^2 \alpha^4 k_e^2 \left[(3.5A + \alpha^2 k_e^2 - \psi^2 k_e^2)^2 + 2.5(\alpha^2 k_e^2 - \psi^2 k_e^2)\right]\omega}{6\pi k_a \left(2A + \alpha^2 k_e^2 - \psi^2 k_e^2\right)^2 \left(A + \alpha^2 k_e^2 - \psi^2 k_e^2\right) A} \tag{26}$$

Equation (26) shows that there is also an optimal resistance, on which the DC electrical power generated by the harvester reaches maximum value. The optimal external resistance for the maximum DC electrical power also changes with the parameters of the harvester, the properties of the piezoelectric material, and the input frequency. Assume that the normalized frequency ψ equals to zero, the optimal resistive load and the maximum generated power can be rewritten as

$$R_{opt2} = \frac{\pi}{2(1 + k_e^2) C_p \omega} \quad \text{and}$$
$$P_{\max 2} = \frac{F_m^2 \left[(3.5 + k_e^2)^2 \alpha^2 + 2.5 k_e^2\right] k_e^2 \omega}{6\pi k_a \alpha^2 (2 + k_e^2)^2 (1 + k_e^2)} \tag{27}$$

Similar with the results from the electromechanical model without rectifier circuit, equation (27) indicates that the maximum harvested DC electrical power is proportional to the input frequency and the square of the amplitude of the external force. Also, the DC electrical power generated by the harvester with a rectified circuit increases with the electromechanical coupling coefficient k_e. For a weak electromechanical coupling coefficient, the optimal resistance can be simplified as $\pi/2C_p\omega$ in this model. Compared equation (27) to equation (16), it can also be found that the optimal external resistive load for the harvester with a rectifier circuit is bigger than the optimal resistance for the harvester without the rectifier circuit. Therefore, it can be concluded that adding a rectifier circuit will cause an increase in the optimal resistance.

Experimental testing

Experimental setup

Figure 5 shows the test specimens of piezoelectric stacks and harvester, whose properties are presented in Table 1. In practice, three rubber layers, which are made up of chloroprene rubber, are used to cover the piezoelectric stacks and protect them from damaging. Parameters and properties of the rubber layer, which were used for simulating the performance of the proposed harvester, are presented in Table 2. The sketch of the test setup is shown in Figure 6 and Figure 7 shows the photo of the test system. As shown in Figure 6, the proposed piezoelectric harvester is installed in a host structure and excited by a spring to evaluate this energy harvesting ability. One side of the host structure is fixed on the ground and another side is connected to the shake table which is used to input the vibration excitations. A spring, as shown in Figure 6, is used to transfer shake table's motions into vibrational force and apply on the harvesting unit.

The test is designed to examine its performance under large-force and low-frequency environments. During the test, the shake table compressed the

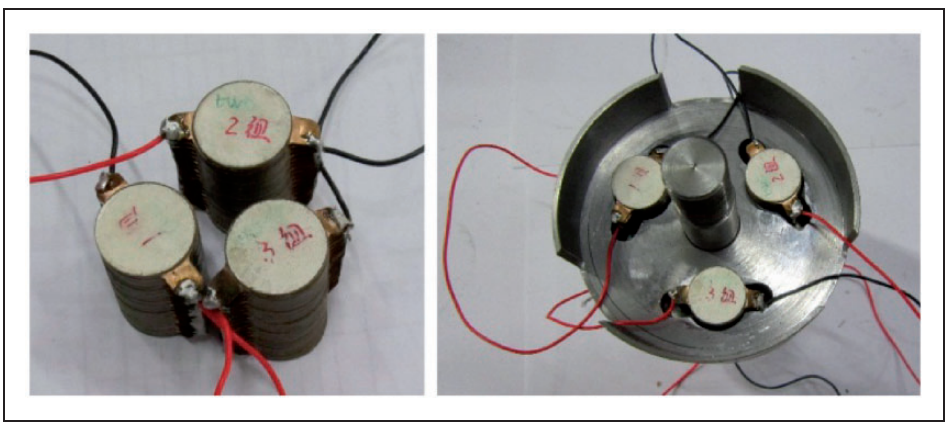

Figure 5. Piezoelectric stacks and harvesting unit.

Table 1. Characteristic properties of the piezoelectric stack.

Material properties	Value	Stack properties	Value
Material type	PZT-8	Diameter (mm)	20
Coupling factors k_{33}	0.68	Height h_p (mm)	34
Piezoelectric constant d_{33} (pC/N)	280	Single wafer thickness t (mm)	0.85
Dielectric constants $\varepsilon_{33}/\varepsilon_0$	1000	Layer number	36
Young's modulus YE_{33} (10^{10} N/m^2)	7.1	Mass m_p (g)	87
Curie point (°C)	320	Capacitance C_p (μF)	0.12
Dissipation factor (%)	0.2	Stiffness k_p (10^9 N/m)	1.1
Density (10^3 kg/m^3)	7.7	Natural frequency ω_n (10^4 rad/s)	11.18

Table 2. Characteristic properties of the rubber layer.

Properties	Value	Properties	Value
Diameter (mm)	20	Height (mm)	3
Young's modulus (10^6 N/m^2)	3.17	Compression modulus (10^6 N/m^2)	231.56
Compression stiffness (10^7 N/m)	8.68	Damping coefficient (N s/m)	192.7

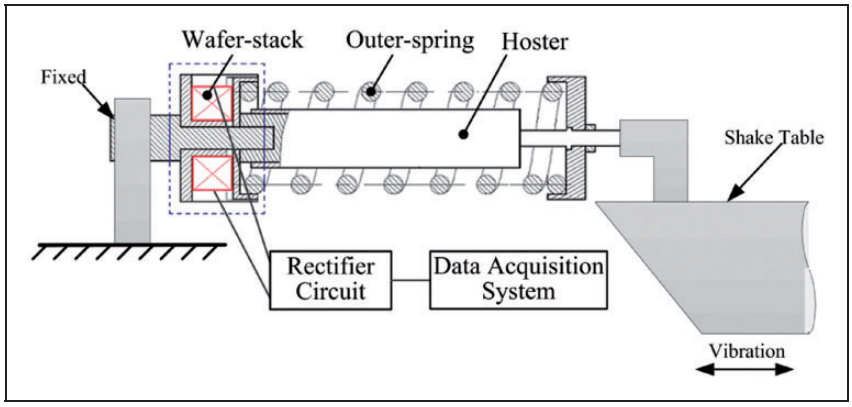

Figure 6. Sketch of the test setup.

outer spring for 50 mm as precompression and then performed different sinusoidal motions with different amplitudes, i.e. 20, 30, and 40 mm, and low frequencies, i.e. 2.0, 4.0, and 6.0 Hz. Shake table motions will be transferred into large force by the spring. A spring with proper stiffness and dimension was chosen to apply exciting force on the harvester. The stiffness of the selected spring was measured to be 34 N/mm using a static compression test. Based on the stiffness of the spring, the maximum force transmitted by the spring reaches 3060 N under maximum amplitude of 40 mm. The harvester generates electrical power when the vibration from the shake table applies on the wafer-stacks. Two series-connected rheostats, as shown in Figure 7, were chosen to serve as the external resistive load of the harvester in order to investigate the relationship between the power output and the electrical resistance. Data acquisition system was

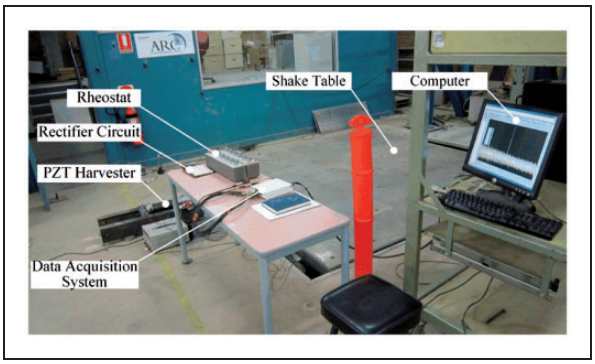

Figure 7. Photo of the test setup.

used to record the output voltage signal applied on the rheostats.

In practice, two kinds of tests (namely AC test and DC test, respectively) were conducted to investigate the

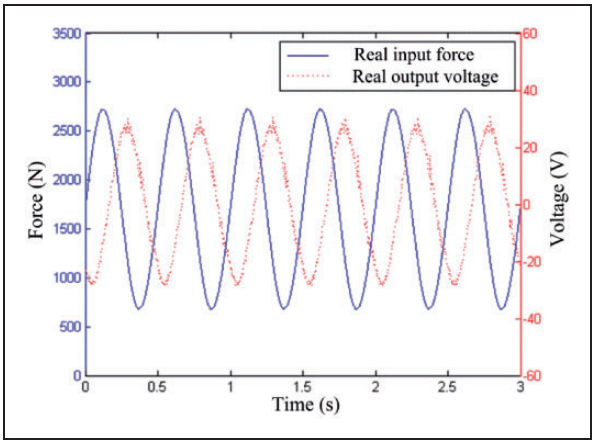

Figure 8. The applied force versus output voltage in AC test.

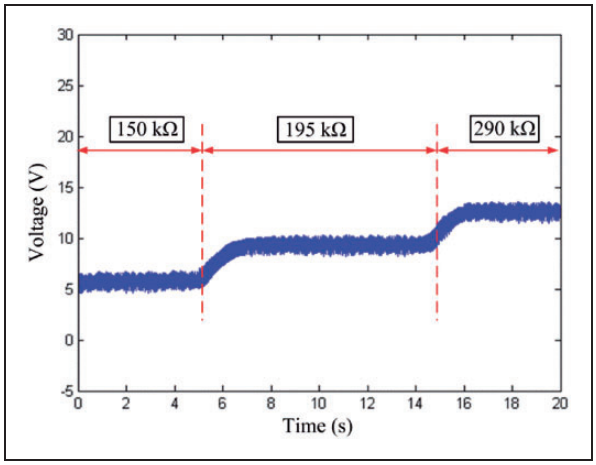

Figure 10. Output voltages in DC test.

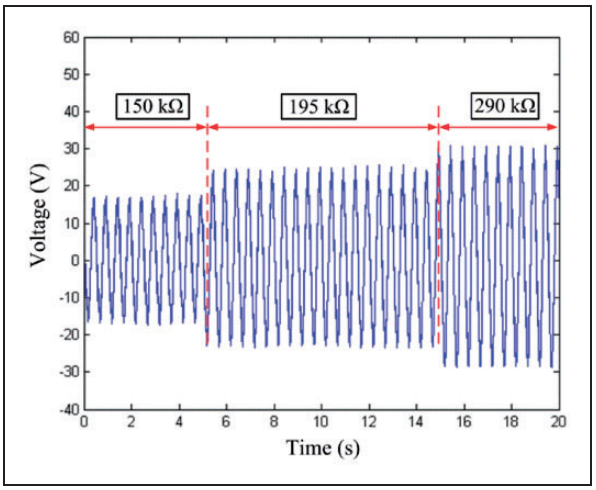

Figure 9. Output voltages in AC test.

performances of the proposed piezoelectric harvester without or with the rectifier circuit. In AC test, the voltages generated by the piezoelectric harvester were directly applied on the external resistive load, i.e. the rheostats; but in DC test, a rectifier circuit between the piezoelectric harvester and the rheostats was used to convert the AC voltages into DC voltages.

Experimental results comparison and discussion

Figure 8 shows the actual force applied on the piezoelectric harvester and the real-time output voltage of the harvester with 290 kΩ resistive load when the shake table performs 30 mm/2 Hz sinusoidal motion. It can be seen that the amplitude of the sinusoidal force applied on the harvester reaches 2600 N. Under this sinusoidal force, the voltage generated by the piezoelectric harvester is AC voltage with the same frequency of the shake table input. Also, as shown in Figure 8, there is a phase change between the applied force and the output AC voltage, which is caused by the response of the outer spring and energy harvesting system itself.

Under the same input, Figures 9 and 10 show the real-time output voltages of the proposed piezoelectric wafer-stack harvester on different electrical resistances in AC test and DC test, respectively. It can be seen from Figure 9 that the voltage output of the harvester, without the rectifier circuit, is an AC voltage and its amplitude increases with the external resistance. Figure 10 shows that the voltage output of the harvester, with the rectifier circuit, is a DC voltage and the value of the DC voltage increases with the external resistance.

Figure 11 shows the relationship between the amplitudes of the voltage/power output in AC test with different external resistive loads under the applied force shown in Figure 8. It can be seen that: (1) the amplitudes of the AC voltage, within a certain range of external resistance, increase with the value of the external resistance, and then trend to constant after the external resistance exceeding a certain value; (2) the amplitudes of the AC power under the external resistance first increase with the resistance, and then trend to decrease after the external resistance exceeding a certain value. There is an optimal resistance, with which the amplitude of the output AC power reaches maximum.

Figure 12 shows the relationship between the DC voltage/power outputs of the harvester with different external resistive loads under the applied force shown in Figure 8. Similar to the results of AC test shown in Figure 11, the output DC voltages vary with the external resistance and there is an optimal resistance, with which the DC power generated by the harvester reaches the maximum.

Comparing Figure 11 with Figure 12, it can be found that the value of optimal resistance in the AC test is higher than that in the DC test under the same shake table input. Figure 13 clearly shows the different optimal resistances of the harvester in the AC and DC test under the same shake table input shown in Figure 8. It can be seen that the optimal resistance for the harvester with the rectifier circuit (about 1050 kΩ)

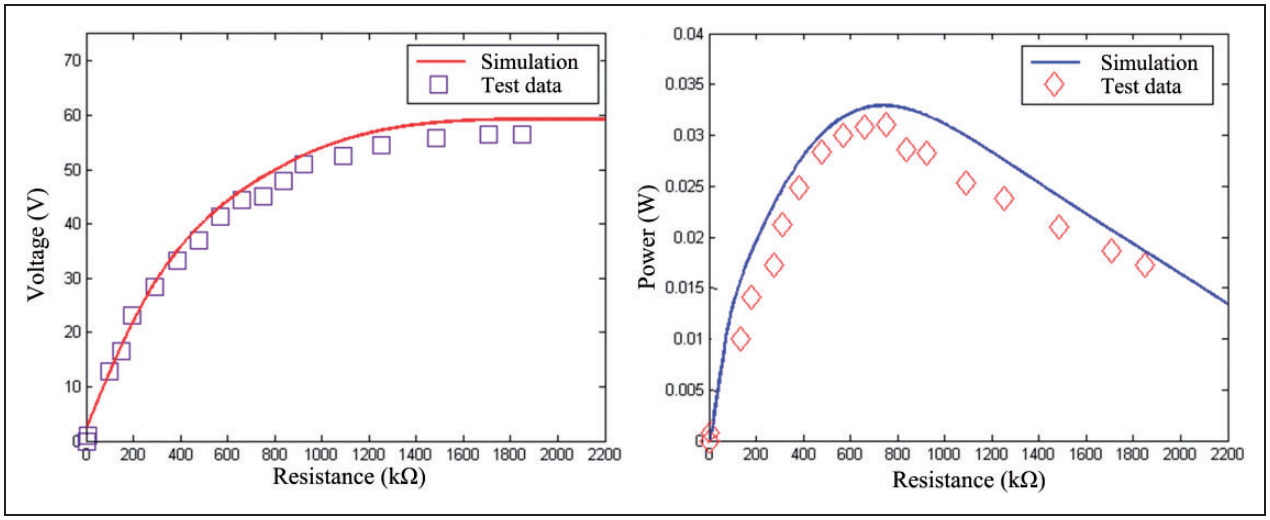

Figure 11. Amplitudes of the AC voltage/power versus resistance under 30 mm/2 Hz testing input.

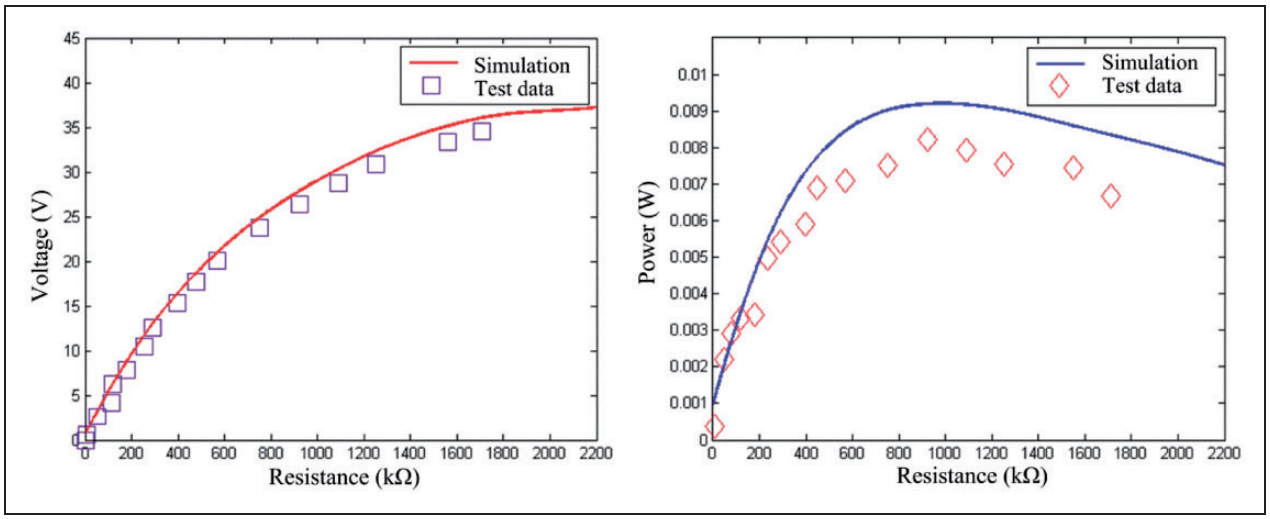

Figure 12. Harvested DC voltage/power versus resistance under 30 mm/2 Hz testing input.

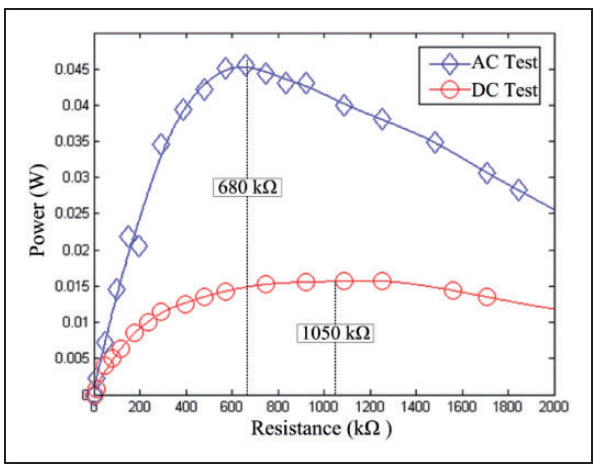

Figure 13. A comparison of the optimal resistance.

is bigger than the optimal resistance for the harvester without the rectifier circuit (about 680 kΩ). This means that adding the rectifier circuit leads to a bigger optimal resistance, which agrees with previous theoretical analysis. Experimental results from Figures 9 to 13 indicate that the external resistive load has a great influence on the electrical power generated by the proposed piezoelectric harvester. Therefore, it is important to find out the optimal resistance in order to maximize the output electrical power under different external vibration excitations.

Figure 14 shows the amplitudes of the output AC power and the DC power under the vibrations with different input amplitudes, i.e. 20, 30, and 40 mm, and fixed frequency, 2 Hz. From Figure 14, it can be seen that: (1) both AC and DC power generated by the harvester increase significantly with the

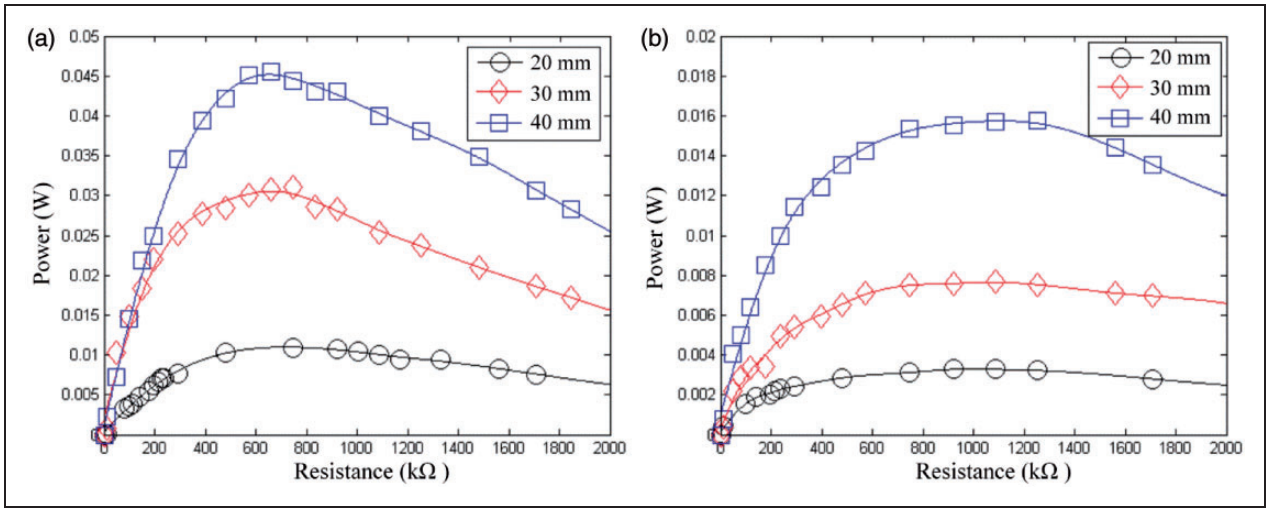

Figure 14. Harvested power comparison under different amplitudes: (a) AC power; (b) DC power.

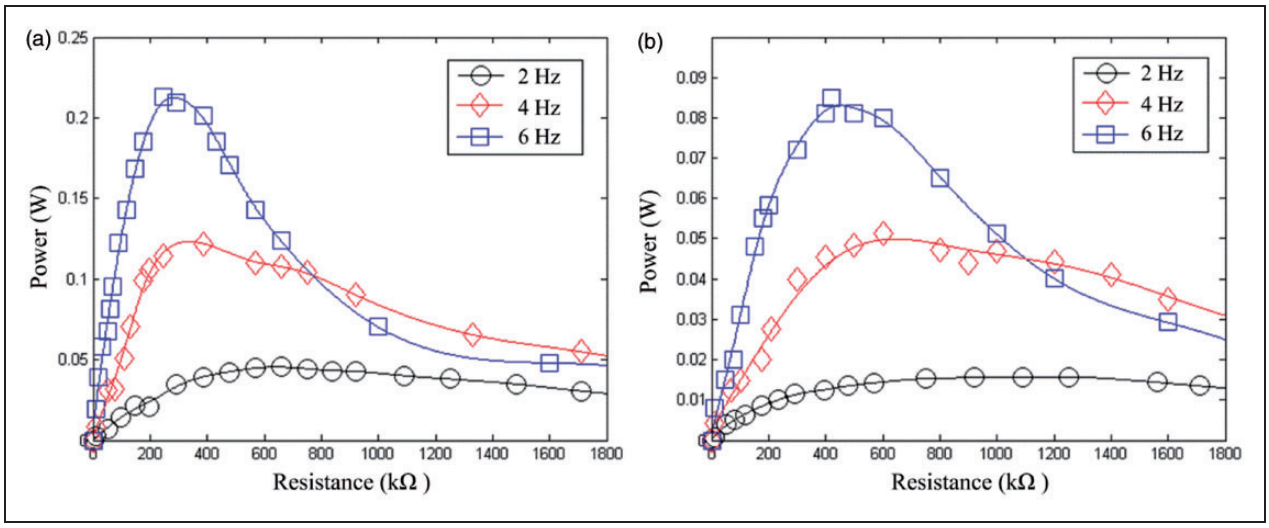

Figure 15. Harvested power comparison under different frequencies: (a) AC power; (b) DC power.

amplitudes of the shake table input. When the input amplitude increases from 20 to 40 mm, the maximum amplitudes of the output AC power and DC power increase from 12 to 45 mW and 3 to 16 mW, respectively (2) the optimal resistance for maximum harvested power does not change with the amplitudes of the force excitations, which agrees with theoretical analysis.

Figure 15 shows the relationships between the harvested powers and the input frequencies of the shake table sinusoidal motions with fixed amplitude, 40 mm, in the AC and DC tests, respectively. It can be seen that: (1) both AC and DC power outputs generated by the harvester increase significantly with the input frequency. When the input frequency increases from 2 to 6 Hz, the maximum amplitudes of the harvested AC power and DC power increase from 45 to 200 mW and 16 to 85 mW, respectively; (2) the optimal resistance for maximum harvested power decreases with the input frequency of the shake table.

Conclusions

This paper presented comprehensive investigations on a compression-based piezoelectric energy harvester for scavenging electrical energy for powering wireless sensor networks in civil and transportation infrastructures. Based on the linear theory of piezoelectricity, this paper presents the theoretical analysis of the piezoelectric multilayer stack harvester, and 2DOF electromechanical models of the proposed harvester (without and with a rectifier circuit) have been developed and examined in this paper. A series of experimental tests were conducted to investigate the performance of the proposed piezoelectric stack harvester and verify the theoretical findings. The experimental results show that the proposed piezoelectric

stack harvester can generate up to 200 mW (AC) and 85 mW (DC) electrical power under harmonic excitation with large force of 3060 N and frequency of 6 Hz, and it is sufficient for powering most normal wireless sensor networks.

Additionally, based on the theoretical analysis and experimental results, the following conclusions can be acquired:

1. The proposed compression-based piezoelectric energy harvester is a linear system, the electrical energy which can be harvested by the proposed vibration harvester increases with the frequency and force amplitude of the harmonic excitation.
2. The electrical power scavenged by the proposed piezoelectric harvester depends not only on the harvester itself but also on the external electrical load. There is an optimal electrical load for a given exciting vibration, with which the electrical power harvested by the harvester reaches maximum value.
3. The optimal electrical load is inversely proportional to exciting frequency, and the value of the optimal electrical load is not affected by the force amplitude of excitation. Under the same input frequency, the optimal electrical load keeps in a constant value for different force amplitudes.

Acknowledgments

Authors would also like to acknowledge the support of the Centre of Built Infrastructure Research, University of Technology, Sydney on the experimental testing part of the project.

Conflict of interest

None declared.

Funding

This work was supported by the National Science Foundation of China under Grant 51175265.

References

1. Cook-Chennault KA, Thambi N and Sastry AM. Powering MEMS portable devices—a review of non-regenerative and regenerative power supply systems with special emphasis on piezoelectric energy harvesting systems. *Smart Mater Struct* 2008; 17: 043001(33pp).
2. Williams CB and Yates RB. Analysis of a micro-electric generator for Microsystems. *Sens Actuat A* 1996; 52: 8–11.
3. Waterbury AC and Wright PK. Vibration energy harvesting to power condition monitoring sensors for industrial and manufacturing equipment. *Proc IMechE, Part C: J Mechanical Engineering Science* 2013; 227: 1187–1202.
4. Harb A. Energy harvesting: State-of-the-art. *Renew Energ* 2011; 36: 2642–2654.
5. Hernandez R, Jung S and Matveev KI. Acoustic energy harvesting from vortex-induced tonal sound in a baffled pipe. *Proc IMechE, Part C: J Mechanical Engineering Science* 2011; 225: 1847–1850.
6. Saadon S and Sidek O. A review of vibration-based MEMS piezoelectric energy harvesters. *Energ Convers Manage* 2011; 52: 500–504.
7. Wischke M, Masur M, Kroner M, et al. Vibration harvesting in traffic tunnels to power wireless sensor nodes. *Smart Mater Struct* 2011; 20: 085014 (8pp).
8. Pasquale GD, Soma A and Fraccarollo F. Piezoelectric energy harvesting for autonomous sensors network on safety-improved railway vehicles. *Proc IMechE, Part C: J Mechanical Engineering Science* 2011; 226: 1107–1117.
9. Xie XD, Wu N, Yuen KV, et al. Energy harvesting from high-risk buildings by a piezoelectric coupled cantilever with a proof mass. *Int J Eng Sci* 2013; 72: 98–106.
10. Roundy S and Wright PK. A piezoelectric vibration based generator for wireless electronics. *Smart Mater Struct* 2004; 13: 1131–1142.
11. Kulah H and Najafi K. Energy scavenging from low-frequency vibrations by using frequency up-conversion for wireless sensor applications. *IEEE Sensors J* 2008; 3: 193–268.
12. Ashraf K, Khir MHM, Dennis JO, et al. Improved energy harvesting from low-frequency vibrations by resonance amplification at multiply frequencies. *Sens Actuat A* 2013; 195: 123–132.
13. Platt SR, Farritor S and Haider H. The use of piezoelectric ceramics for electric power generation within orthopaedic implants. *IEEE/ASME Trans Mechatronics* 2005; 10: 455–461.
14. Keawboonchuay C and Engel TG. Design, modelling, and implementation of a 30-kW piezoelectric pulse generator. *IEEE Trans Plasma Sci* 2002; 30: 679–686.
15. Keawboonchuay C and Engel TG. Scaling relationships and maximum peak power generation in a piezoelectric pulse generator. *IEEE Trans Plasma Sci* 2004; 32: 1879–1885.
16. Feenstra J, Granstrom J and Sodano H. Energy harvesting through a backpack employing a mechanically amplified piezoelectric stack. *Mech Syst Signal Pr* 2008; 22: 721–734.
17. Brainerd JG, Jensen AG, Cumming LG, et al. Standards on piezoelectric crystals. *Proceedings of the I. R. E.* 1949; 37: 1378–1395.
18. Smits JG. Iterative method for accurate determination of the real and imaginary parts of the materials coefficients of piezoelectric ceramics. *IEEE Trans Sonics Ultrason SU* 1976; 23: 393–402.